Slab-geometry Nd:glass laser performance studies

J. M. Eggleston,* T. J. Kane, J. Unternahrer,† and R. L. Byer

Applied Physics Department, Edward L. Ginzton Laboratory of Physics, Stanford University, Stanford, California 94305

Received May 10, 1982

Slab-geometry solid-state lasers potentially provide significant performance improvements relative to conventional rod-geometry lasers. We have used a Nd:glass laser test-bed facility to verify the predicted slab-configuration advantages.

Solid-state lasers have been traditionally fabricated in the form of pencil-like rods. Under thermal loading, these host rods manifest optical distortions, which include thermal focusing, stress-induced birefringence, and stress-induced biaxial focusing.[1-4] These effects can severely degrade the optical quality of the laser output at medium pump powers and completely extinguish laser oscillation at high pump powers.

The concept of a slab laser geometry with a zigzag optical path confined in the slab by total internal reflection was first proposed by Martin and Chernoch in 1972.[5] The advantages of this approach include the elimination of stress-induced birefringence and biaxial focusing in large volumes of pumped material.[6] Only recently has the promise of slab-configuration solid-state lasers been realized.[7,8]

In this Letter we present experimental measurements that used a Nd:glass test-bed slab laser. The results are compared with computer-model predictions of the slab-geometry approach. The computer model calculates and displays the temperature and stress fields in the slab and from these predicts birefringence and index-of-refraction distributions. The effect of these distributions on optical propagation is determined in a polarization-sensitive ray-tracing section of the model. Stress-induced surface curvature and the resulting focusing effects are also calculated.

Figure 1(a) is a schematic of a Brewster-angle-cut slab in a laser resonator. The pump light enters the slab through polished faces, which allow total internal reflection of the optical beam. These faces are in direct contact with the coolant. The unpumped faces are normally uncooled so that the temperature distribution nearly approximates a slab of infinite extent. The flashlamp reflector structure, shown in an end view in Fig. 1(b), is designed for uniform illumination of the slab. The slab is mounted in a holder (shown by the crosshatched regions) that seals by an O ring within the flashlamp reflector housing, thus permitting rapid exchange of the glass slab.

The slab geometry creates a natural axis of symmetry for stresses that are independent of position except near the uncooled edges. Thus, if the polarization direction is aligned with the symmetry directions, the stress-induced birefringence does not lead to depolarization in the central region of the slab. The computer-model-predicted depolarization of a He–Ne probe beam propagating through the slab is shown in Fig. 2(a). The dark areas indicate regions of maximum depolarization. Note that the central region extends to within one slab thickness of the edge. The details of the depolarization pattern are due to the rotation of stress tensor axes near the slab corners and to residual depolarization remaining after the zigzag optical-path averaging of the birefringence.[9]

Figure 2(b) shows a comparison of the measured and predicted depolarization along the width line w shown in Fig. 2(a). The slab is pumped by 1600 W of average flashlamp power, of which 6.3%, or 100 W, is assumed to be dissipated as thermal energy in the slab. The measured and predicted depolarization is in agreement for a thermal-heat loading that is 1.9 times the average power stored in the upper laser level. Because of the finite spatial resolution, the peaks and valleys of the depolarization are not fully resolved.

Depolarization measurements made traversing the slab along the thickness line t are shown in Fig. 2(c). Again, the agreement between the measured depolarization and computer-model-predicted depolarization is excellent. The actual and modeled powers into the slab are the same as in Fig. 2(b). It should be noted that the slab fractures for average pump power into the flashlamps of 2 kW. A rod system under similar pumping conditions would exhibit multiple-waveplate phase shifts, which in turn would lead to complete depolarization of the laser beam.

In a slab, which is theoretically infinite in the x di-

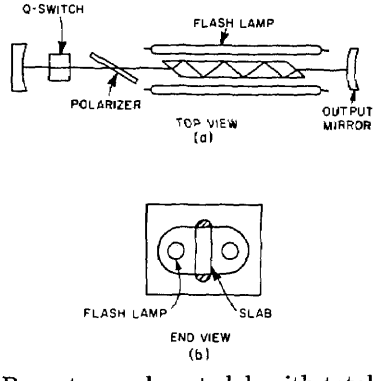

Fig. 1. (a) Brewster-angle-cut slab with total-internal-reflection zigzag optical path in a Q-switched unstable-resonator oscillator. (b) End view of the slab showing the flashlamp within the flooded reflector structure.

0146-9592/82/090405-03$1.00/0

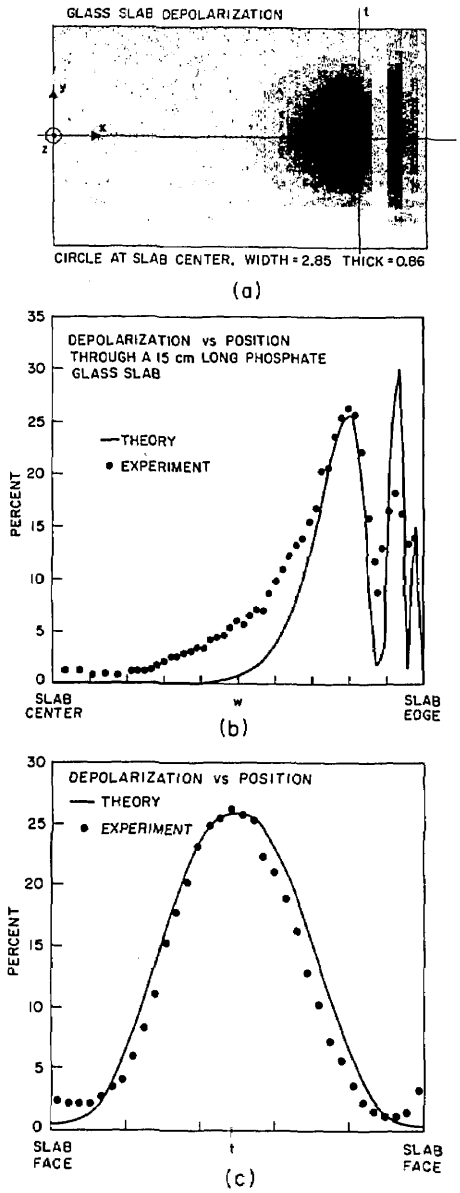

Fig. 2. (a) Computer-model-predicted slab depolarization for a He–Ne probe beam for a 1600-W average-power flashlamp-pumped 15-cm-long by 2.5-cm-wide by 0.83-cm-thick slab. 100 W, or 6.3% of the flashlamp average power, is assumed to be dissipated as thermal energy in the slab. (b) Measured (dots) and predicted (solid line) depolarization versus position along line w and (c) along line t, which passes through the region of peak depolarization. The depolarization averaged over the entire slab volume is less than 2%.

rection, the zigzag path eliminates the first-order focusing effects arising from the thermal- and stress-induced cylindrical lensing. In a finite slab, end effects and distortions of the total internal reflection surfaces give rise to first-order focusing effects. Both the end effects and surface distortions are induced by thermal loading of the slab and are sensitive to the details of the slab cooling. The measured focal lengths using the test-bed slab laser system are less than predicted by the computer model. However, the focusing is not biaxial and is correctable by thin-lens cylindrical elements in the resonator of the present system. The focusing was found to vary linearly with average pump power. For example, the focal lengths at the 1600-W pump level are 6 and 4 m in the x and y directions, respectively, at the center of the slab. By contrast, for a rod pumped at the stress-fracture limit, the stress-induced biaxial focusing has an average focal length of 1.14 m and is not correctable by a lens element.

The optical quality of the slab test-bed laser was measured by probing the slab with a He–Ne laser, propagating to the far field, and evaluating the far-field diffraction pattern. The beam was diffraction limited for probe-beam diameters up to 6 mm. The beam quality of the slab test-bed laser was also verified by observing the output-beam profile of both an unstable resonator oscillator[10,11] and a radial birefringent resonator oscillator[12,13] in the near field. The tenth-wave optical quality of the glass and the near-tenth-wave fabrication flatness of the total internal reflecting glass surfaces yield a significantly better optical quality transverse mode than can be achieved in widely used Nd:YAG unstable-resonator laser systems.

The laser performance of the test-bed system was also measured. The slab was pumped by two flashlamps with a (PFN) that delivered up to 300 J of energy per lamp in a 170-μsec-long pulse. The xenon-filled flashlamps had a 15-cm arc length and a 9-mm internal diameter. SCR switching was used in a simmered discharge configuration to achieve low switching noise and long lamp life. The energy and power extraction for the slab in a stable-resonator configuration with a 30% output coupler is shown in Fig. 3(a). The average storage efficiency for the 3.5% Nd-doped slab, defined as the percentage of lamp energy deposited in the upper laser level, was determined to be 3.3%. This number is based on a gain measurement averaged over the slab volume and the known cross section of LHG5 phosphate glass.[14] Ground-state absorption losses that are due to thermal population of the lower laser level of 5% per pass lead to a 2% slope efficiency and 1.6% extraction efficiency, where the extraction efficiency is defined as the ratio of the laser output energy to the energy stored in the PFN.

The average power into the slab was held to 1600 W to avoid fracturing the slab. The average output power was 25 W when the entire volume of the slab was used. The average output power can be increased by increasing either the length or the width of the slab.

The slab was also operated in an unstable-resonator configuration with a magnification of 1.75 and a mode diameter of 5.2 mm. In this configuration the system was operated in both long-pulse and Q-switched modes. A comparison of the output energies achieved is shown in Fig. 3(b). Since the flashlamp discharge time was less than the upper-state lifetime of 240 μsec, the Q-switched and normal pulse energies are comparable. The Q-switched energy for this mode volume was limited by the available flashlamp energy and by the onset of optical component damage threshold near the 4-J/cm^2 circulating optical fluence in the resonator.

The oscillator output was redirected and amplified in an unused portion of the slab, which resulted in an output energy of 1.2 J per pulse. This energy was frequency doubled in preliminary experiments in a KD*P crystal with 25% efficiency. Both the second-harmonic and the fundamental beams were Raman shifted in a

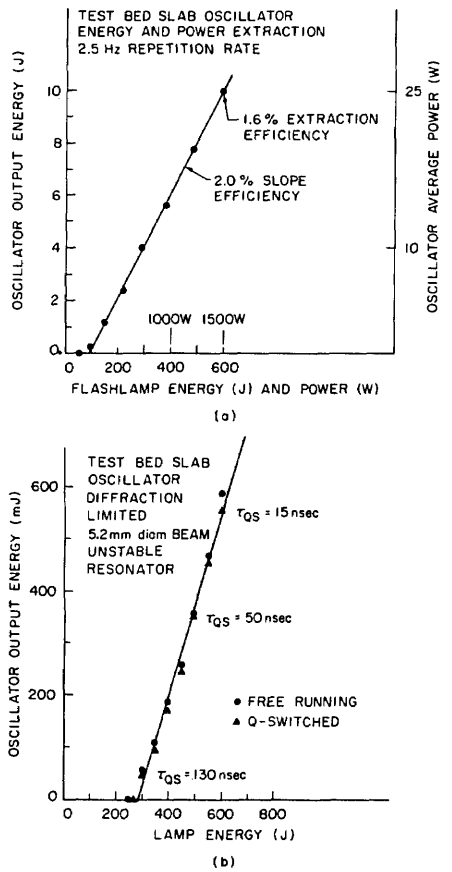

Fig. 3. (a) Oscillator output energy and average output power extracted from the test-bed oscillator operating at 2.5-Hz repetition rate in a long-pulse mode with 30% output coupler. The round-trip loss that is due to lower-laser-level absorption was measured to be 10%, which led to a lower slope-efficiency value compared with storage efficiency. (b) Q-switch oscillator output energy from a $M = 1.75$ unstable resonator with a 5.2-mm beam diameter. The diffraction-limited output energy was limited by the selected mode volume, the flashlamp energy, and the approach to the optical-component damage threshold near 4/J/cm^2 circulating fluence.

1-m cell filled with 30 atm of hydrogen gas. These experiments provided an indirect verification of the spatial-mode quality of the laser beam.

The current test-bed laser system was designed to allow experimental verification of the computer model and is not an optimum design. The performance was limited by the 15-cm slab length, which in turn limited the gain to values less than optimum. The thermal-induced stress of the 8.3-mm-thick slab limited the repetition rate to 5 Hz. A more optimized slab of 30-cm length at 6 mm-thickness would allow operation at the multiple-joule level at a 10-Hz repetition rate. In addition, the system efficiency could be improved by a more efficient reflector structure and by the use of more highly doped glasses.

In conclusion, we have used a test-bed slab Nd:glass laser system to demonstrate the predicted advantages of the slab configuration of reduced depolarization and thermal- and stress-induced focusing. The measurements are in good agreement with the computer-model predictions. The slab configuration offers significant laser-performance advantages compared to the traditional rod-laser geometry.

We acknowledge the assistance of K. Kuhn for second-harmonic and Raman measurements and the support provided by the U.S. Army Reseach Office under grant #DAAG29-81-C-0038, the U.S. Department of Energy under grant #DOE3818301, and the National Aeronautics and Space Administration under grant #NAG1-182. J. M. Eggleston would like to acknowledge the support of the Fannie and John K. Hertz Foundation.

* Mathematical Sciences Northwest, Bellevue, Washington.

† Swiss Institute of Nuclear Research, Villingen, Switzerland.

References

1. G. D. Baldwin and E. P. Reidel, "Measurements of dynamical optical distortion in Nd-doped glass laser rod," J. Appl. Phys. **38**, 2726 (1967).
2. L. M. Osterink and J. D. Foster, "Thermal effects and transverse mode control in a Nd:YAG laser," Appl. Phys. Lett. **12**, 128 (1968).
3. J. D. Foster and L. M. Osterink, "Thermal effects in a Nd:YAG laser," J. Appl. Phys. **41**, 3656 (1970).
4. W. Koechner, "Thermal lensing in a Nd:YAG laser rod," Appl. Opt. **9**, 2548 (1970).
5. W. S. Martin and J. P. Chernoch, "Multiple internal reflection face pumped laser," U.S. Patent 3,633,126 (1972).
6. W. B. Jones, L. M. Goldman, and J. C. Almasi, "Performance characteristics of two face pumped face cooled glass lasers," Tech. Rep. AFAL-TR-72-233 (General Electric Research and Development, Schenectady, N.Y., 1972).
7. Y. S. Liu, W. B. Jones, and J. P. Chernoch, "Recent development of high power visible laser sources employing solid state slab lasers and nonlinear harmonic conversion techniques," Rep. 81CRD104 (General Electric Research and Development, Schenectady, N.Y., 1981).
8. R. L. Byer, T. Kane, and J. M. Eggleston, "Solid state laser sources for remote sensing," presented at the Monterey Remote Sensing Conference, Monterey, California, February 1982; see also "Slab geometry solid state lasers," in *Digest of Conference on Lasers and Electro-Optics* (Optical Society of America, Washington, D.C., 1982).
9. T. J. Kane, J. M. Eggleston, and R. L. Byer, "Polarized cw Nd:YAG laser using a slab geometry," in *Digest of Conference on Lasers and Electro-Optics* (Optical Society of America, Washington, D.C., 1982).
10. R. L. Herbst, H. Komine, and R. L. Byer, "A 200 mJ unstable resonator Nd:YAG oscillator," Opt. Commun. **21**, 5 (1977).
11. W. B. Jones, "Faced pumped laser with diffraction limited output beam," U.S. Patent 4,214,216 (1980).
12. G. Giuliani, Y. K. Park, and R. L. Byer, "Radial birefringent element and its application to laser resonator design," Opt. Lett. **5**, 491 (1980).
13. J. M. Eggleston, G. Giuliani, and R. L. Byer, "Radial intensity filters using radial birefringent elements," J. Opt. Soc. Am. **71**, 1264 (1981).
14. S. E. Stokowski, R. A. Saroyan, and M. J. Weber, "Nd-doped laser glass spectroscopic and physical properties," in *Laser Glass Handbook* (U.S. Department of Energy, Washington, D.C., 1978), no. LLNL-M-95.